Cancer Immunol Immunother (2012) 61:215–221
DOI 10.1007/s00262-011-1184-2

SHORT COMMUNICATION

Hypericin-based photodynamic therapy induces surface exposure of damage-associated molecular patterns like HSP70 and calreticulin

Abhishek D. Garg · Dmitri V. Krysko · Peter Vandenabeele · Patrizia Agostinis

Received: 25 August 2011 / Accepted: 4 December 2011 / Published online: 23 December 2011

Abstract Surface-exposed HSP70 and calreticulin are damage-associated molecular patterns (DAMPs) crucially involved in modulating the success of cancer therapy. Photodynamic therapy (PDT) involves the administration of a photosensitising (PTS) agent followed by visible light-irradiation. The reactive oxygen species that are thus generated directly kill tumours by damaging their microvasculature and inducing a local inflammatory reaction. PDT with the PTS photofrin is associated with DAMPs exposure, but the same is not true for other PTSs. Here, we show that when cancer cells are treated with hypericin-based PDT (Hyp-PDT), they surface-expose both HSP70 and calreticulin (CRT). Induction of CRT exposure was not accompanied by co-exposure of ERp57, but this did not compromise the ability of the exposed CRT to regulate the phagocytosis of Hyp-PDT-treated cancer cells by dendritic cells. Interestingly, we found that Hyp-PDT-induced CRT exposure (in contrast to anthracycline-induced CRT exposure) was independent of the presence of ERp57. Our results indicate that Hyp-PDT is a potential anti-cancer immunogenic modality.

Keywords Calreticulin · HSP70 · Photodynamic therapy · Hypericin · Cancer · DAMPs

Abbreviations

CNTR	Control(s)
DAMP(s)	Damage-associated molecular pattern(s)
DC	Dendritic cells
Ecto-CRT	Surface externalised-calreticulin
Ecto-HSP70	Surface externalised-Heat shock protein 70
ER	Endoplasmic reticulum
HSP	Heat shock proteins
Hyp-PDT	Hypericin-based photodynamic therapy
MTX	Mitoxantrone
PDT	Photodynamic therapy
PTS(s)	Photosensitiser(s)

Introduction

Damage-associated molecular patterns (DAMPs) were recently identified as an important set of molecules mediating crucial processes such as immunogenic apoptosis [1–5]. Recent studies have shown that photodynamic therapy (PDT), a well-established anti-tumour modality [6], effectively generates several DAMPs [7–9]. Heat shock proteins (HSPs), and especially HSP70, are the best characterised DAMPs associated with PDT [8, 10]. Photofrin-PDT causes exposure of HSP70 (ecto-HSP70) on the surface of treated cells [8, 11], and this ecto-HSP70 plays an important role in opsonisation of cancer cells [12]. Recently, it was reported that photofrin-PDT promotes surface exposure of calreticulin (ecto-CRT) [13]. Ecto-CRT, a well-characterised ‘eat

Electronic supplementary material The online version of this article (doi:10.1007/s00262-011-1184-2) contains supplementary material, which is available to authorized users.

A. D. Garg · P. Agostinis (✉)
Cell Death Research and Therapy Unit, Department of Molecular Cell Biology, Faculty of Medicine, Catholic University of Leuven, Campus Gasthuisberg O&N1, Herestraat 49, 3000 Leuven, Belgium
e-mail: patrizia.agostinis@med.kuleuven.be

D. V. Krysko · P. Vandenabeele
Molecular Signaling and Cell Death Unit, Department for Molecular Biomedical Research, VIB, Ghent, Belgium

D. V. Krysko · P. Vandenabeele
Department of Biomedical Molecular Biology, Ghent University, Ghent, Belgium

me' signal [3, 14], has recently emerged as a key mediator of the immunogenicity of dying tumour cells [3].

Most research on PDT-induced DAMP exposure has been done with photofrin as a photosensitiser (PTS) [7, 8, 10]. However, since surface exposure of DAMPs seems to be modulated by stress occurring in particular organelles, such as the endoplasmic reticulum (ER) [15], PTSs that localise to different subcellular sites can be tested for efficient DAMP exposure in a PDT setup [10]. To this end, we used hypericin-based PDT (Hyp-PDT). This procedure uses the PTS hypericin, which associates dominantly with the ER membranes [16]. In this setup, we investigated the induction of ecto-HSP70 and ecto-CRT, which represent a well-studied DAMP and a new DAMP [5], respectively.

Materials and methods

Cell lines and treatments

T24, CT26 and MEF cells were cultured at 37°C under 5% CO_2 in DMEM cell culture medium. The JAWSII murine dendritic cell (DC) line was cultured in RPMI 1640 medium supplemented with 5 ng/ml granulocyte macrophage-colony stimulating factor (GM-CSF, PeproTech, Rocky Hill, NJ, USA) as described [16]. For induction of anthracycline-based CRT surface exposure, the cells were treated with mitoxantrone (MTX; 1 μM; Sigma, St. Louis, MO, USA) for 4 h. Unless otherwise mentioned, for Hyp-PDT, T24 and CT26 cells were incubated with 150 nM hypericin (for 16 h in serum-containing medium) whereas MEF cells were incubated with 200 nM hypericin (for 2 h in serum-free medium). Hypericin was prepared, purified and stored as described [16]. Irradiation was performed as described [17]. Four Hyp-PDT doses based on light fluence were defined as low (0.54 J/cm^2), medium (1.35 J/cm^2), high (2.16 J/cm^2) and highest (2.7 J/cm^2). Cells loaded with hypericin were handled either in the dark or under subdued light (<1 μW/cm^2). All the control samples (CNTR or untreated) were incubated with hypericin but were not irradiated. CT26 cells (treated with highest PDT dose) were analysed on FACSCalibur after staining with DAPI (Molecular Probes) for cell viability determination and annexin-V-FITC (BD Biosciences) for assessment of phosphatidylserine exposure.

In vitro phagocytosis assay

JAWS II DCs were labelled with 1 μM Cell tracker Green (Invitrogen, Merelbeke, Belgium) as described [18]. CT26 or MEF cells were harvested 1 h after exposure to a high or medium dose of Hyp-PDT, respectively, or left untreated (CNTR). MEF cells were labelled with 1.5 μM Cell tracker CM-Dil during this recovery interval (Invitrogen, Merelbeke, Belgium). In certain experiments, CT26 cells were coated either with 2 μl/10^6 cells of isotype control (Chicken IgY; Abcam, Cambridge, UK) or with chicken anti-CRT antibody (Abcam, Cambridge, UK) for 30 min at 37°C. They were then co-cultured with JAWS II DCs for 2 h at 37°C at a ratio of 1:5 (JAWSII:CT26). Phagocytosis was assessed by flow cytometry (FACSCalibur, Beckton & Dickinson, Mountain View, CA, USA). The percentage of double-positive phagocytes was calculated according to the following formula: 100 × number of double-positive cells/(single-positive + double-positive cells). Contour pictograms were plotted using the FlowJo software (Tree Star, Ashland, OR, USA).

Cell surface protein biotinylation

This procedure was performed as described [3, 15]. Isolation of plasma membrane proteins was confirmed by detecting FAS exclusively in the plasma membrane preparations. Time points used for this analysis were confirmed to be associated with non-significant plasma membrane permeabilisation via LDH release assay (data not shown).

Immunoblotting

Determination of protein concentration and immunoblotting were done as described [17]. Immunoblotting was done with primary antibodies against ERp57, HSP90 (Cell Signaling Technology, Danvers, MA, USA), calreticulin (anti-CRT) (Stressgen, Victoria, BC, Canada), actin (Sigma, St. Louis, MO, USA), PARP (BD Pharmingen, San Jose, CA, USA), FAS/CD95 (N-18, M-20 and C-20) and HSP70 (Santa Cruz Biotech, Santa Cruz, CA, USA). Secondary antibodies conjugated to horseradish peroxidase were purchased from Cell Signaling Technology (Danvers, MA, USA).

Cell surface CRT and HSP70 fluorescence detection

For surface immunofluorescence analysis, T24 cells were fixed in 4% paraformaldehyde, incubated with either anti-CRT (Affinity Bioreagents, Golden, CO, USA) or anti-HSP70 antibodies (Santa Cruz Biotech), and then with the IgG antibody conjugated with Alexa fluor 488 (Invitrogen, Carlsbad, CA, USA). Fluorescence was evaluated with a FluoView FV1000 Confocal Laser-scanning microscope (Olympus).

Phagocytosis motif search

Phagocytosis motif search was performed manually by aligning the phagocytosis-assisting motifs, NPxY and RGD [19], with individual protein sequences using ClustalW2 software (http://www.ebi.ac.uk/Tools/msa/clustalw2/) with default settings to reject alignments with gaps.

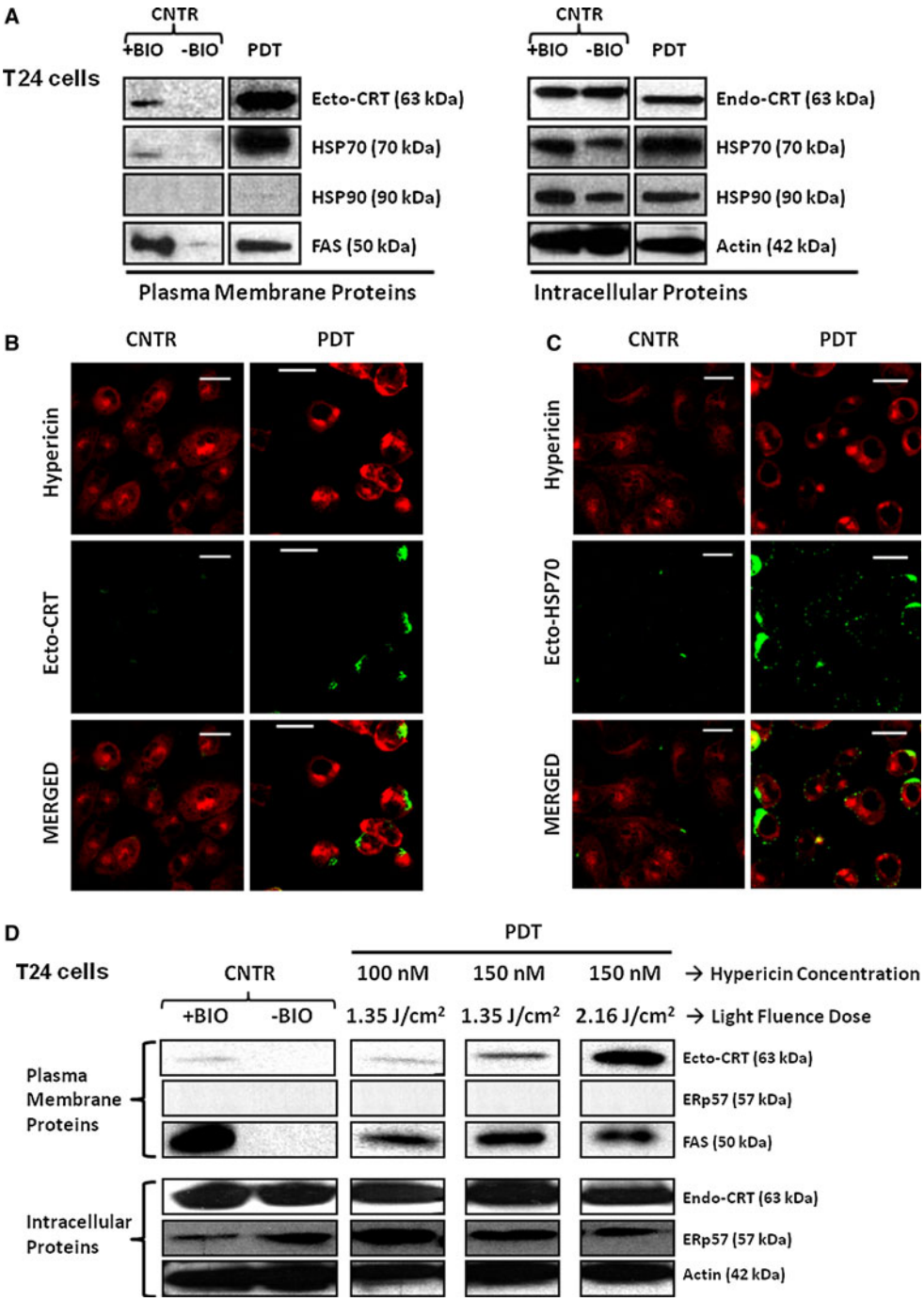

Fig. 1 Hypericin-PDT-treated cancer cells surface-expose HSP70 and calreticulin but not ERp57. **a** T24 cells were treated with high PDT dose followed by surface protein biotinylation at 1 h post-PDT and immunoblotted. **b**, **c** T24 cells were treated with high PDT dose, fixed and surface immunostained at 1.5 h post-PDT for either CRT (**b**) or HSP70 (**c**) such that extranuclear fluorescence of residual hypericin was also visualised (*scale bar* = 20 μm). **d** T24 cells were incubated with 100 nM or 150 nM hypericin for 16 h and irradiated at a fluency of either 1.35 or 2.16 J/cm^2. This was followed by surface protein biotinylation at 2 h post-PDT and immunoblotting. CNTR denotes untreated samples. Furthermore, '+BIO' indicates controls exposed to buffer with biotin and '−BIO' indicates controls exposed to buffer without biotin. Representative Western blots are shown for three independent experiments

Results

Hypericin-PDT causes enhanced surface exposure of calreticulin and HSP70 on cancer cells

To determine whether Hyp-PDT-treated cancer cells surface-expose HSP70 and CRT, we performed surface protein biotinylation analysis [3] on PDT-treated as well as untreated (CNTR) T24 human bladder carcinoma cells (Fig. 1). This revealed that Hyp-PDT caused considerable enhancement in surface exposure of both CRT (Fig. 1a) and HSP70 (Fig. 1a) in absence of HSP90 surface exposure. In fact, this ecto-CRT and ecto-HSP70 exposure occurred as soon as 30 min after PDT (Online resource 1). Ecto-CRT (Fig. 1b) and ecto-HSP70 (Fig. 1c) on Hyp-PDT-treated cells could also be detected by immunofluorescence staining. Interestingly, ecto-CRT was mostly present in unevenly distributed patches on the cell surface (Fig. 1b), as observed previously [3, 14]. On the other hand, ecto-HSP70 tended to be present both as patches and

as small clumps, but it was relatively more evenly distributed on the cell surface (Fig. 1c).

Hypericin-PDT-induced ecto-CRT is not accompanied by surface co-translocation or dependent on ERp57

Recent research has shown that CRT is co-translocated from the ER lumen to the cellular surface as a complex with ERp57 [3, 20], a member of the protein disulphide isomerase (PDI) family, which is crucial for surface tethering of ecto-CRT [20]. On the other hand, no such surface co-translocated protein complex has been implicated in surface tethering of ecto-HSP70 [8, 11, 21]. Considering the importance of ERp57/CRT complex formation for surface exposure of this DAMP, we decided to further explore the surface exposure behaviour of Hyp-PDT-induced ecto-CRT. After Hyp-PDT, cancer cells exposed CRT in the absence of ERp57 (Fig. 1d). Ecto-CRT induced by Hyp-PDT was dependent on the hypericin concentration as well as on the light dose. A light fluence of 1.35 J/cm^2 induced more ecto-CRT at 150 nM hypericin than at 100 nM (Fig. 1d). At 150 nM hypericin, the dose of 2.16 J/cm^2 produced more ecto-CRT than the dose of 1.35 J/cm^2 (Fig. 1d).

Next, we tried to analyse whether the absence of ERp57 affects the induction of ecto-CRT by Hyp-PDT. In wild-type (WT) MEF cells, both mitoxantrone (MTX) and Hyp-PDT induced ecto-CRT, as expected (Fig. 2a). MTX is a type II topoisomerase inhibitor that causes ERp57-dependent ecto-CRT induction [3, 15]. In line with published data [20], MEF cells lacking ERp57 (ERp57 KO MEFs) did not show ecto-CRT after MTX treatment (Fig. 2a). However, cells that were treated with Hyp-PDT were still able to surface-expose CRT despite the absence of ERp57 (Fig. 2a).

Surface-exposed CRT (independent of ERp57) assists in phagocytosis of Hyp-PDT-treated cancer cells

Since Hyp-PDT-induced ecto-CRT was not accompanied by ecto-ERp57, it was important to determine whether absence of ecto-ERp57 compromises the functionality of the ecto-CRT 'eat me' signal [3, 14] after Hyp-PDT. An in silico analysis (phagocytosis motif search) revealed that two motifs in CRT (NPEY and KGE) are closely homologous to the two most important phagocytosis-assisting motifs, NPxY and RGD [19] (Fig. 2b). This analysis showed that ecto-CRT, when present, has the motifs needed to assist in phagocytosis. Moreover, we observed that contrary to previous observations [22], in the case of Hyp-PDT, absence of ERp57 (KO) did not reduce the phagocytosis of Hyp-PDT-treated cells (in comparison with ERp57 competent WT cells) by JAWSII murine dendritic cell (DC) line (Online resource 2) [23]. Next, we investigated the effect of ecto-CRT on phagocytosis of Hyp-PDT-treated CT26 tumour cells in vitro. As observed earlier for T24 cells, Hyp-PDT induced ecto-CRT exposure in absence of ERp57 surface exposure in CT26 cells as well (Fig. 2c). It should be noted that Hyp-PDT was capable of causing CT26 cell death (Fig. 2d). In fact, Hyp-PDT-treated CT26 cells were phagocytosed efficiently by the JAWSII DCs within a few hours after treatment (Fig. 2e). Moreover, blockade of ecto-CRT by a specific anti-CRT antibody reduced this phagocytosis (Fig. 2e). We used an avian anti-CRT antibody because it does not interact with the mouse Fc receptors [3].

Fig. 2 Hypericin-PDT induces ERp57-independent ecto-CRT that regulates phagocytosis of PDT-treated cells. **a** MEF cells containing ERp57 (WT) or lacking it (KO) were treated with a medium PDT dose (recovered, 1 h post-PDT), MTX (1 μM for 4 h) or left untreated (CNTR). This was followed by surface protein biotinylation and immunoblotting. **b** CRT, HSP70 and HSP90 were analysed for the presence of homologous sequences representing the phagocytic motifs (NPxY and RGD) with respect to positive controls (MFG-E8 and Annexin-1) and negative control (Actin). In parentheses are the respective homologous sequences for each protein. **c** CT26 murine tumour cells were treated with high PDT dose followed by surface protein biotinylation at 1 h post-PDT and immunoblotting. **d** CT26 cells were treated with PDT or left untreated (CNTR) and recovered 24 h post-PDT followed by staining with annexin-V-FITC and the vital dye 4,6-diamidino-2-phenylindole (DAPI). **e** Hypericin-labelled CT26 cells treated with PDT were incubated with chicken anti-CRT or isotype antibody, followed by detection of phagocytosis by Cell Tracker Green (CTGr)-labelled JAWSII DCs. JAWSII cells accumulated in quadrant I (no phagocytosis) and quadrant II (phagocytic uptake) while free CT26 cells accumulated in quadrant III. Calculated % phagocytosis is mentioned for the respective pictograms. Results are representative of two independent experiments with two replicates in each. Furthermore in **a** and **c**, '+BIO' indicates controls exposed to buffer with biotin and '−BIO' indicates controls exposed to buffer without biotin. Representative Western blots are shown for three independent experiments

Discussion

Only a few anti-cancer therapies (anthracyclines, MTX and photofrin-PDT) can induce exposure of both ecto-HSP70 and ecto-CRT [8, 13, 21]. We show that hypericin-based PDT [16] is another modality that can accomplish this (Fig. 1). By contributing to the small arsenal of anti-cancer agents that can induce surface exposure of DAMPs, our study has possible implications for anti-tumour immunology.

We also report the existence of slight differences between the surface distribution patterns of ecto-HSP70 (Fig. 1c) and ecto-CRT (Fig. 1b). The peculiarly patchy distribution of ecto-CRT plays an important role in its phagocytosis-regulating functions [14]. Moreover, we found that ERp57 was not surface co-exposed with ecto-CRT [20] after Hyp-PDT (Figs. 1d, 2c). Interestingly, a

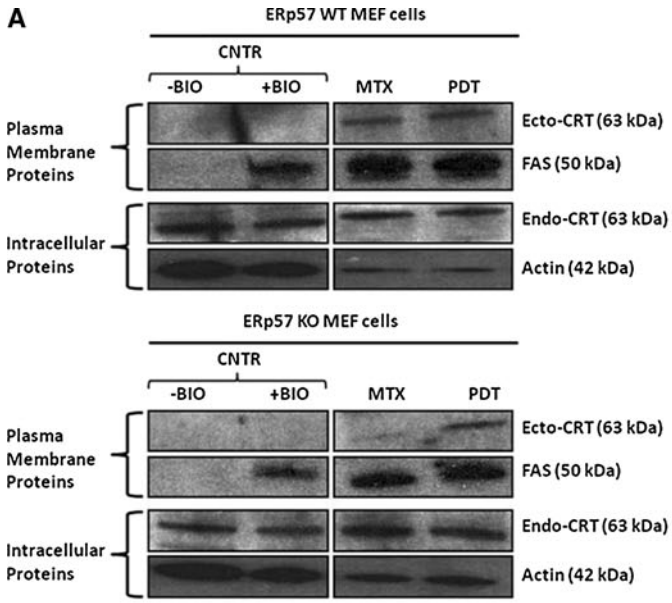

B

Phagocytic Motifs	DAMPs	Positive Controls	Non-DAMP Controls
Presence	CRT *(NPEY, KGE)*	MFG-E8 *(NPSY, RGD)*, Annexin-A1 *(KPAF, -)*	None
Absence	HSP70, HSP90	None	Actin

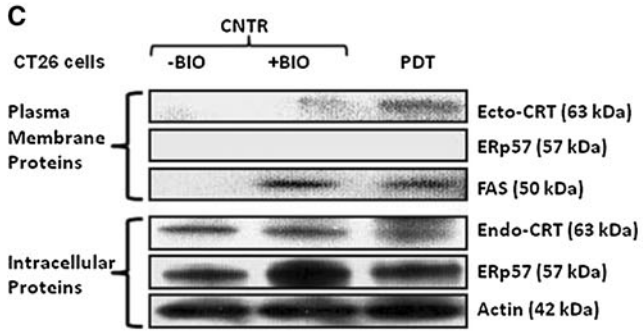

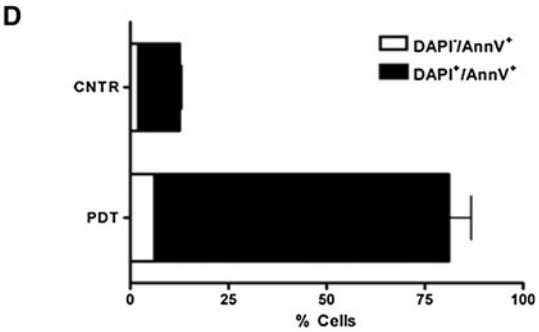

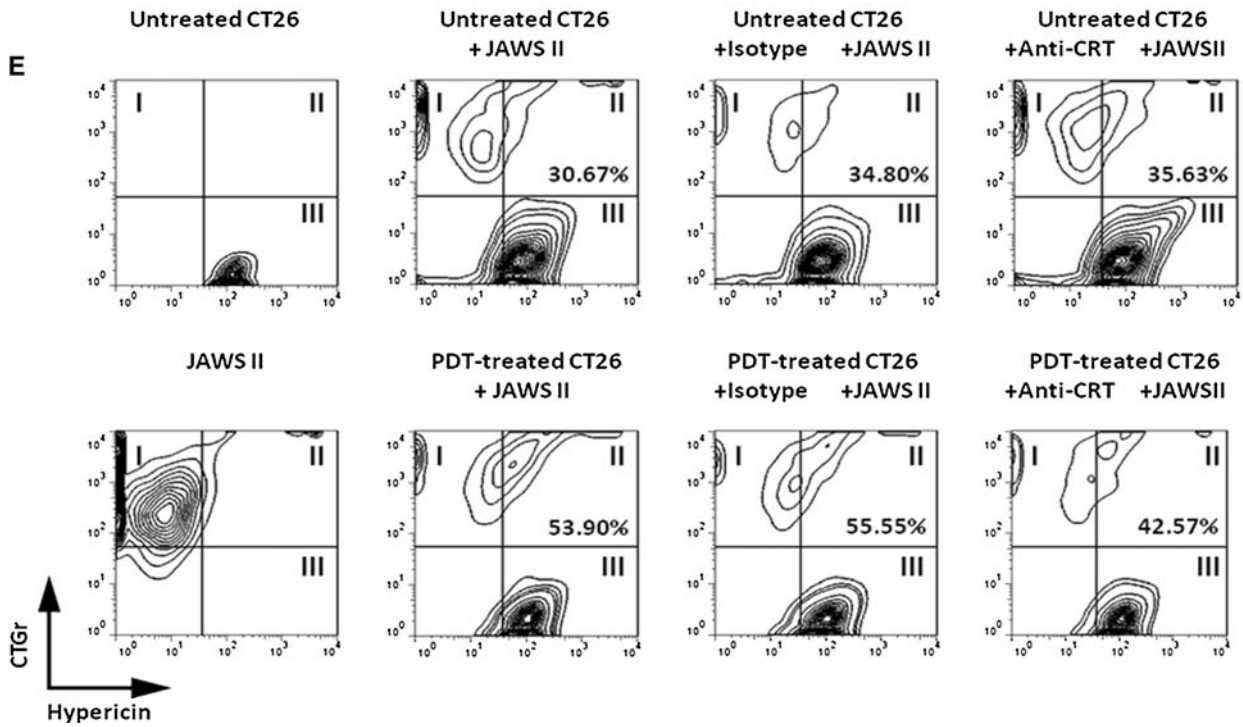

recent study has shown that surface co-translocation of ERp57 is also dispensable for thapsigargin-induced ecto-CRT [24]. Thus, our study implies that ERp57 surface exposure is probably not a universal phenomenon and might apply mainly to anthracyclines, MTX and UVC irradiation [3, 20].

However, the absence of surface-exposed ERp57 did not compromise the phagocytosis-assisting capabilities of ecto-CRT, and antibody-based blocking of ecto-CRT reduced the phagocytosis of Hyp-PDT-treated cancer cells (Fig. 2e). However, this reduced phagocytosis after ecto-CRT blockade was still higher than control levels thereby pointing towards the possible presence of other phagocytosis-assisting factors. It would be important to identify these factors in future. Furthermore, our in silico analysis shows that CRT contains motifs homologous to the phagocytosis-assisting motifs [19], NPxY and RGD (Fig. 2b). On the other hand, HSP70 and HSP90, which are also surface-exposed DAMPs, do not have such homologous sequences (Fig. 2b). This observation is substantiated by a recent observation indicating that the increase in phagocytosis correlates better with the amount of ecto-CRT than the amount of ecto-HSP70 or ecto-HSP90 [21].

A recent study has shown that absence of ERp57 abrogates MTX-induced ecto-CRT [20]. We confirm that observation (Fig. 2a). However, Hyp-PDT-induced ecto-CRT (and by extension phagocytosis after Hyp-PDT treatment) was not reduced by the absence of ERp57 (Fig. 2a, e). Interestingly, we observed that % phagocytosis for untreated MEFs (Online resource 2) was higher than for untreated CT26 cells (Fig. 2e), which represents a possible cell line–to–cell line difference in basal phagocytosis observable across other studies [3, 14, 24]. Thus, this is the first study describing ERp57-independent CRT exposure. Our finding is intriguing because ERp57 has been suggested to play an important role in the (anthracycline/MTX-induced) ecto-CRT translocation pathway [15, 20]. It would be interesting to investigate whether Hyp-PDT-induced ecto-CRT follows a different molecular pathway to reach the cell surface.

Hyp-PDT induces surface exposure of HSP70 and CRT in cancer cells. Thus, it is a potential anticancer modality for eliciting ‘emission’ of immuno-modulatory DAMPs. Further studies are needed to identify other surface-exposed or secreted DAMPs that are induced by Hyp-PDT in cancer cells.

Acknowledgments We thank Dr. Peter Carmeliet (Vesalius Research Center, VIB, Leuven, Belgium) for the CT26 cells and Dr. Natalio Garbi (German Cancer Research Center, Heidelberg, Germany) for the ERp57 WT and KO MEF cells. This work was supported by a project from the Fund for Scientific Research Flanders (FWO-Vlaanderen, G.0728.10 to P.A. and D.V.K). Research in Agostinis’ group is supported by grants from the K.U.Leuven (GOA/11/009) and FWO-Vlaanderen (G.0661.09). This paper presents research results of the IAP6/18, funded by the Interuniversity Attraction Poles Programme, initiated by the Belgian State, Science Policy Office. D.V.K. is paid by a fellowship from FWO-Vlaanderen. Research in Vandenabeele’s group is supported by VIB and Ghent University (GROUP-ID consortium of the UGent MRP initiative), FWO-Vlaanderen (G.0875.11 and G.0973.11), Federal Research Program (IAP 6/18), European Research Program FP6 ApopTrain (MRTN-CT-035624), FP7 Apo-Sys 200767, and the Euregional PACTII. P.V. holds a Methusalem grant (BOF09/01M00709) from the Flemish Government. We thank Jan Piessens for the technical support. We also thank Dr. Esther Buytaert for her help and contribution to the experiments. We would like to thank Dr. Amin Bredan for excellent editing of the manuscript.

Conflict of interest The authors declare that they have no conflict of interest.

References

1. Krysko DV, Agostinis P, Krysko O, Garg AD, Bachert C, Lambrecht BN, Vandenabeele P (2011) Emerging role of damage-associated molecular patterns derived from mitochondria in inflammation. Trends Immunol 32(4):157–164. doi:10.1016/j.it.2011.01.005
2. Bianchi ME (2007) DAMPs, PAMPs and alarmins: all we need to know about danger. J Leukoc Biol 81(1):1–5. doi:10.1189/jlb.0306164
3. Obeid M, Tesniere A, Ghiringhelli F, Fimia GM, Apetoh L, Perfettini JL, Castedo M, Mignot G, Panaretakis T, Casares N, Metivier D, Larochette N, van Endert P, Ciccosanti F, Piacentini M, Zitvogel L, Kroemer G (2007) Calreticulin exposure dictates the immunogenicity of cancer cell death. Nat Med 13(1):54–61. doi:10.1038/nm1523
4. Zitvogel L, Kepp O, Kroemer G (2010) Decoding cell death signals in inflammation and immunity. Cell 140(6):798–804. doi:10.1016/j.cell.2010.02.015
5. Garg AD, Nowis D, Golab J, Vandenabeele P, Krysko DV, Agostinis P (2010) Immunogenic cell death, DAMPs and anticancer therapeutics: an emerging amalgamation. Biochim Biophys Acta 1805(1):53–71. doi:10.1016/j.bbcan.2009.08.003
6. Agostinis P, Berg K, Cengel KA, Foster TH, Girotti AW, Gollnick SO, Hahn SM, Hamblin MR, Juzeniene A, Kessel D, Korbelik M, Moan J, Mroz P, Nowis D, Piette J, Wilson BC, Golab J (2011) Photodynamic therapy of cancer: an update. CA Cancer J Clin 61(4):250–281. doi:10.3322/caac.20114
7. Korbelik M, Stott B, Sun J (2007) Photodynamic therapy-generated vaccines: relevance of tumour cell death expression. Br J Cancer 97(10):1381–1387. doi:10.1038/sj.bjc.6604059
8. Korbelik M, Sun J, Cecic I (2005) Photodynamic therapy-induced cell surface expression and release of heat shock proteins: relevance for tumor response. Cancer Res 65(3):1018–1026. doi:65/3/1018
9. Garg AD, Nowis D, Golab J, Agostinis P (2010) Photodynamic therapy: illuminating the road from cell death towards anti-tumour immunity. Apoptosis 15(9):1050–1071. doi:10.1007/s10495-010-0479-7
10. Garg AD, Krysko DV, Vandenabeele P, Agostinis P (2011) DAMPs and PDT-mediated photo-oxidative stress: exploring the unknown. Photochem Photobiol Sci 10(5):670–680. doi:10.1039/c0pp00294a
11. Zhou F, Xing D, Chen WR (2008) Dynamics and mechanism of HSP70 translocation induced by photodynamic therapy treatment. Cancer Lett 264(1):135–144. doi:10.1016/j.canlet.2008.01.040

12. Korbelik M, Sun J (2006) Photodynamic therapy-generated vaccine for cancer therapy. Cancer Immunol Immunother 55(8):900–909. doi:10.1007/s00262-005-0088-4
13. Korbelik M, Zhang W, Merchant S (2011) Involvement of damage-associated molecular patterns in tumor response to photodynamic therapy: surface expression of calreticulin and high-mobility group box-1 release. Cancer Immunol Immunother. doi:10.1007/s00262-011-1047-x
14. Gardai SJ, McPhillips KA, Frasch SC, Janssen WJ, Starefeldt A, Murphy-Ullrich JE, Bratton DL, Oldenborg PA, Michalak M, Henson PM (2005) Cell-surface calreticulin initiates clearance of viable or apoptotic cells through trans-activation of LRP on the phagocyte. Cell 123(2):321–334. doi:10.1016/j.cell.2005.08.032
15. Panaretakis T, Kepp O, Brockmeier U, Tesniere A, Bjorklund AC, Chapman DC, Durchschlag M, Joza N, Pierron G, van Endert P, Yuan J, Zitvogel L, Madeo F, Williams DB, Kroemer G (2009) Mechanisms of pre-apoptotic calreticulin exposure in immunogenic cell death. EMBO J 28(5):578–590. doi:10.1038/emboj.2009.1
16. Buytaert E, Callewaert G, Hendrickx N, Scorrano L, Hartmann D, Missiaen L, Vandenheede JR, Heirman I, Grooten J, Agostinis P (2006) Role of endoplasmic reticulum depletion and multidomain proapoptotic BAX and BAK proteins in shaping cell death after hypericin-mediated photodynamic therapy. FASEB J 20(6):756–758. doi:10.1096/fj.05-4305fje
17. Vantieghem A, Assefa Z, Vandenabeele P, Declercq W, Courtois S, Vandenheede JR, Merlevede W, de Witte P, Agostinis P (1998) Hypericin-induced photosensitization of HeLa cells leads to apoptosis or necrosis. Involvement of cytochrome c and procaspase-3 activation in the mechanism of apoptosis. FEBS Lett 440(1–2):19–24. doi:S0014-5793(98)01416-1
18. Krysko DV, Denecker G, Festjens N, Gabriels S, Parthoens E, D'Herde K, Vandenabeele P (2006) Macrophages use different internalization mechanisms to clear apoptotic and necrotic cells. Cell Death Differ 13(12):2011–2022. doi:10.1038/sj.cdd.4401900
19. Singh S, D'Mello V, van Bergen en Henegouwen P, Birge RB (2007) A NPxY-independent beta5 integrin activation signal regulates phagocytosis of apoptotic cells. Biochem Biophys Res Commun 364(3):540–548. doi:10.1016/j.bbrc.2007.10.049
20. Panaretakis T, Joza N, Modjtahedi N, Tesniere A, Vitale I, Durchschlag M, Fimia GM, Kepp O, Piacentini M, Froehlich KU, van Endert P, Zitvogel L, Madeo F, Kroemer G (2008) The co-translocation of ERp57 and calreticulin determines the immunogenicity of cell death. Cell Death Differ 15(9):1499–1509. doi:10.1038/cdd.2008.67
21. Fucikova J, Kralikova P, Fialova A, Brtnicky T, Rob L, Bartunkova J, Spisek R (2011) Human tumor cells killed by anthracyclines induce a tumor-specific immune response. Cancer Res 71(14):4821–4833. doi:10.1158/0008-5472.CAN-11-0950
22. Obeid M (2008) ERP57 membrane translocation dictates the immunogenicity of tumor cell death by controlling the membrane translocation of calreticulin. J Immunol 181(4):2533–2543
23. Taborda CP, Casadevall A (2002) CR3 (CD11b/CD18) and CR4 (CD11c/CD18) are involved in complement-independent antibody-mediated phagocytosis of Cryptococcus neoformans. Immunity 16(6):791–802. doi:S107476130200328X
24. Peters LR, Raghavan M (2011) Endoplasmic reticulum calcium depletion impacts chaperone secretion, innate immunity, and phagocytic uptake of cells. J Immunol 187(2):919–931. doi:10.4049/jimmunol.1100690